RAPID COMMUNICATIONS

PHYSICAL REVIEW A VOLUME 44, NUMBER 3 1 AUGUST 1991

Measurement of absolute rates for multiphoton ionization of atomic hydrogen at 248 nm

George A. Kyrala and T. David Nichols
Physics Division, Los Alamos National Laboratory, Los Alamos, New Mexico 87545
(Received 12 March 1991)

We present measurements of absolute rates for multiphoton ionization of the ground state of atomic hydrogen by a linearly polarized, subpicosecond KrF laser at a wavelength of 248 nm. The irradiance was varied from 3×10^{12} to 2×10^{14} W/cm^2, and three above-threshold-ionization peaks were observed. The measured rate for total electron production was less than that predicted by Floquet theory [S.-I. Chu and J. Cooper, Phys. Rev. A **32**, 2769 (1985)] and perturbation calculations [S. V. Khristenko and S. I. Vetchinkin, Opt. Specktrosc. **40**, 239 (1976)], but significantly higher than calculated by the Reiss [Phys. Rev. A **22**, 1786 (1980)] and Keldysh [Sov. Phys. JETP **20**, 1307 (1965)] methods using Volkov final states.

The interaction of atomic hydrogen with an intense laser field is a fundamental test of the features of multiphoton ionization and above threshold ionization (ATI) without the complications of multielectron effects. Several theoretical calculations of multiphoton ionization of atomic hydrogen have been published [1–12]. There are simple perturbative calculations that include intermediate states to some order [2–5,9,10] and those that employ Volkov states as the final states without including any intermediate states [1,6,8]. There are also calculations that simulate the atom-radiation field by Floquet states [7], and time-dependent three-dimensional calculations with direct numerical integrations of the Schrödinger equation [11,12]. These calculations for the simple hydrogen atom differ by as much as 3 orders of magnitude at a given irradiance. Due to their simplicity, Volkov-state Keldysh-Faisal-Reiss (KFR) models are widely used in calculations of plasma heating by multiphoton ionization [13]. It is necessary to measure the absolute accuracy of these ionization rates to check the validity of using KFR models to calculate their contribution to plasma heating.

Very few experiments have been performed on the multiphoton ionization of atomic hydrogen [14–17]. Only one group [14] has measured an absolute ionization rate. The others were interested primarily in the Stark shift [15], ionization by two applied radiation fields [16], or angular distributions of the resulting electrons [17]. The rate that was measured could not be compared directly to theoretical predictions, because the laser field was multimode. This increased the ionization rate by a factor which could not be measured, but which was estimated to be 6!, or 720.

This paper presents a crossed beam measurement of the absolute rates for three-photon nonresonant ionization of atomic hydrogen by 248-nm linearly polarized light. Figure 1 shows the energy diagram of the system with a schematic of the expected signal. Two main features of this experiment are the few-photon nature of the process and the absence of intermediate excited states that shift into resonance during the irradiation. The photoionization process, and the models that describe it, are therefore uncomplicated. In order to avoid the problem of Ref. [14], the longitudinal modes of the laser beam were mode locked, with a pulse length near the transform limit. This indicates that the irradiance had a smooth temporal profile without the high-irradiance spikes typical of chaotic multimode beams. Thus there is no enhancement of the ionization rate compared to a single-mode beam.

The photoelectrons originated at the intersection of an atomic hydrogen beam and a focused laser beam. Figure 2 is a schematic diagram of the interaction region. In this figure, the hydrogen beam flows from top to bottom, the laser beam points out from the page, and the electron spectrometer extends to the right. Atomic hydrogen from an rf discharge source [18] was collimated by a 1-mm-diam Teflon coated skimmer to form the atomic beam. The skimmer also acted as a differential pumping aperture between the source region and the interaction region. The density of hydrogen atoms was measured with a quadrupole residual-gas analyzer (RGA) and agreed with estimates from the measured gas flow rate.

An electron time-of-flight (TOF) spectrometer with a 2π-sr collection angle was used to distinguish between electrons from hydrogen atoms and those from molecules

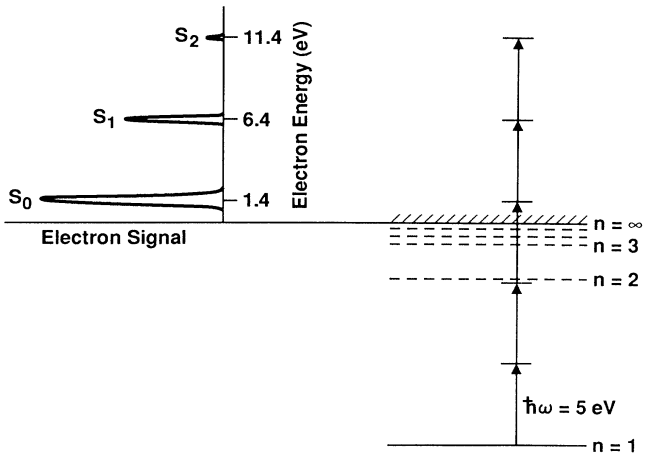

FIG. 1. Simplified energy-level diagram of a hydrogen atom showing schematically electron peaks from absorption of three, four, and five 5-eV KrF photons.

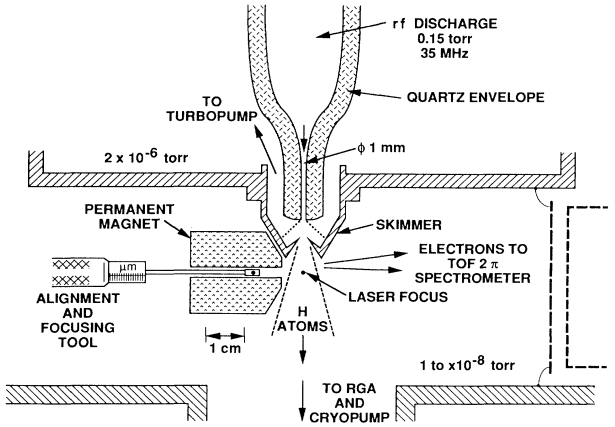

FIG. 2. Schematic diagram of the interaction region. The laser beam is orthogonal to this view.

of hydrogen and water. The electron spectrometer was based on the Kruit and Read magnetic bottle design [19], but used a permanent magnet rather than an electromagnet. The electrons were detected by a microchannel plate (MCP) 1.087 m from the interaction region. The total number of electrons produced in the interaction region was calculated from the MCP signal, the detection efficiency of the MCP, the transparencies of the grids, the collection angle of the spectrometer, and the average signal recorded when single electrons were incident on the MCP. A small fraction of the electrons in the H peaks arose from multiphoton ionization of H_2 and its products:

$$\begin{aligned} H_2+4h\nu &\rightarrow H+H^+ + e(1.91\text{ eV}) \\ &\quad +h\nu \\ &\quad \downarrow \\ &\quad H^+ + H^+ + e(1.91\text{ eV}) + e(1.4\text{ eV}) . \end{aligned}$$

Another small fraction was from photoelectrons from the grids at the entrance of the spectrometer. The background from the grid electrons did not depend on the gas pressure and their spectrum was simply subtracted. The photoionization signals were measured separately by turning off the rf discharge and varying the density of H_2. To isolate the atomic contribution, we modulated the H signal by turning the discharge on and off. We scaled the discharge-off spectrum such that the amplitudes of the molecular peaks at 4.5 eV were the same as that in the discharge-on case. We then subtracted the scaled spectrum from the discharge-on case. In this way the H_2 contribution in the resulting spectrum was eliminated.

The laser has been described previously [20]. During these measurements, its output energy was typically 25 mJ with a pulse length of 600 ± 50-fsec full width at half maximum (FWHM), as determined by two-photon ionization of NO with an assumed $\text{sech}^2(t)$ shape. The product of the temporal and spectral widths was two to three times the product for a transform limited pulse. A diffraction-limited, 50 mm diam, $f/20$ off-axis parabolic mirror focused the laser beam to a spot at the center of the interaction region. The laser beam exited through a beam dump channel and was collected by a joulemeter so that each electron spectrum could be averaged with others of the same pulse energy. The width of each energy bin was 3% of the mean energy.

The peak irradiance at the center of the interaction region was adjusted over the range 3×10^{12} to 2×10^{14} W/cm^2, corresponding to peak ponderomotive potentials of 0.02–1.1 eV, with beam splitters and reflective neutral-density filters. This method of attenuation changed the pulse shape and irradiance distribution as little as possible, especially since the spot size was larger than the diffraction-limited spot size. The sensitivity of the collected electron spectra to movement of the laser focus was tested by translating the focusing mirror in three dimensions. There was no change in the spectra for displacements smaller than 200 μm from the point of maximum signal, and considerably larger displacements were possible in most directions. This tolerance results from the large difference among the characteristic dimensions of the focal spot, the atomic beam, and the magnetic field of the spectrometer. It was also noted that variations in electron count that occurred from time to time with a single configuration of the attenuation chain were frequently greater than variations due to replacement of the attenuators. Therefore, the scatter in measured electron counts at a single measured irradiance is not due primarily to the method of attenuation, but to changes in factors such as the waist radius of the laser beam.

Peak irradiance was determined from the total energy of each laser pulse, the pulse length, and the average radius of the beam waist, which was measured to be 35 ± 2 μm under normal conditions. Occasionally, the waist radius grew to 45 μm, or varied between these values. Since the radius was not measured during the collection of electron spectra, these occasions must be recognized by the decrease in electron production rates. Calculated peak irradiances were checked against the ponderomotive shift of the electron energies, which indicated the irradiance at which the ionization occurred. This was possible because the time required for an electron to leave the focal volume was much greater than the duration of the laser pulse. The ponderomotive shift was too small to measure when the irradiance was less than 10^{13} W/cm^2, but higher irradiances calculated by this method agreed with the others within the estimated uncertainties. At the highest irradiance, the maximum ponderomotive shift, 0.56 ± 0.08 eV, correspond not to the highest irradiance of the laser pulse, but to a value of $1.0 \pm 0.5 \times 10^{14}$ W/cm^2. This is interpreted as the irradiance at which the last atom in the high-irradiance region was ionized. Irradiances at points other than the beam waist were determined by fitting an M^2 model [21] to measured beam diameters at different distances from the focusing mirror. In this model, the radius of a beam that contains transverse modes changes with distance along the axis (z) more quickly than a TEM_{00} beam of the same waist radius (W_0). The actual radius $W(z)$ can be described by the equation

$$[W(z)]^2 = W_0^2 \left[1 + \left(\frac{M^2 \lambda z}{\pi W_0^2} \right)^2 \right]$$

where $M^2 = 1$ for a TEM_{00} beam, $\lambda = 248$ nm, and $z = 0$ at

the waist. For each value of z, the irradiance at a distance $W(z)$ from the axis is less than that on the axis by a factor of $1/e^2$. The fitted value of M^2 was 6.2 ± 1, indicative of the effect of the amplifier's gain on the spatial distribution.

In order to compare the experimental results with the theoretical calculations, the calculations were folded with the experimental parameters to predict a signal. The focal volume was divided into shells along contours of equal peak irradiance, so that all atoms within a shell experience the same temporal history. Some shells were truncated at the edge of the atomic beam. Within each shell, the theoretical ionization rates were integrated over the temporal shape of the laser pulse to find the number of electrons released. The sum over the entire focal volume was compared to the measured signal.

Figure 3 shows the measured electron counts compared to several models. Each curve has been normalized to a density of 10^{10} atoms/cm^3. The low-irradiance measurements were actually taken at this density, but the density was reduced to 10^9 atoms/cm^3 for the high-irradiance cases to avoid space-charge effects. The lowest theoretical curves represent the Keldysh [1] and Reiss [6] models using Volkov final electron states. The model closest to the measured points is the Keldysh model including the factor that Keldysh derived to account for the Coulomb field of the ion in the final state [1]. The next higher curve represents the Floquet theory of Chu and Cooper [7]. The highest curve [3] is typical of perturbation calculations, which differ from each other by as much as a factor of three. The numerical integration models are not included because the tabulations presently do not include ionization rates at irradiances less than 10^{13} W/cm^2. The total electron count is very sensitive to these rates because of the large volume of hydrogen in the low-irradiance wings.

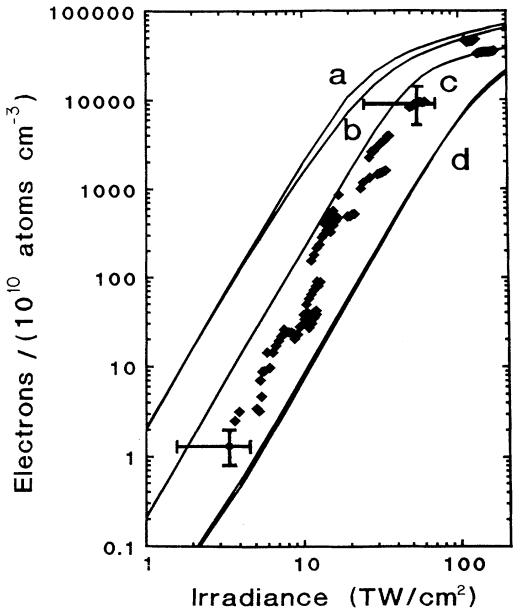

FIG. 3. Comparison of measured electron production rates to theoretical rates: *a*, Perturbative (Ref. 3); *b*, Floquet (Ref. 7); *c*, Coulomb-corrected Keldysh (Ref. 1); and *d*, Keldysh (Ref. 1) and Reiss (Ref. 6). Measurements are shown as unconnected points. Each set is normalized to a hydrogen atom density of 10^{10} cm^{-3}

The error bars in Fig. 3 are "worst case" estimates, assuming that all errors are in the same direction. The uncertainty in normalized electron count is thus $+62-43\%$, and the uncertainty in irradiance is $+30-54\%$. The uncertainty in irradiance includes the possibility that the waist radius at any time might be 30% larger than the ideal case, which makes the error bars strongly asymmetric. The uncertainty in electron count was mostly due to the electron detection efficiency ($\pm 20\%$) and the measurement of gas density ($\pm 20\%$).

Each curve in Fig. 3 increases with irradiance I approximately as I^3 until the electron count reaches 10000. At this point, a significant fraction of the atoms in the focal volume have been ionized, and the rate of growth decreases. The dependence of the highest electron counts comes chiefly from expansion of the low-irradiance wings of the focus. It differs from the familiar $I^{1.5}$ rule for a cylindrically symmetric beam [22] because of the finite size of the atomic beam. It is often useful to locate the point at which the electron count versus irradiance curve "breaks," then apply simple approximations to check the consistency of the various measurements. In this experiment, the relatively low slope of the curve, compared to those involving infrared and visible lasers, together with relatively large uncertainties in the measured points, prevents precise location of the break point. Still, one can reasonably say that it lies between 40 and 120 TW/cm^2, thus agreeing with the ponderomotive shift results. One rule, presented in Ref. [14], is that $N_e = N_H V_3$, where N_e is the number of electrons at the break, N_H is the density of hydrogen atoms, and V_3 is an effective focal volume for a three-photon process, accounting for the finite size of the atomic beam. Taking N_H as 10^{10} atoms/cm^3, this rule estimates N_e as 30000, corresponding to 120 TW/cm^2 in Fig. 3. Another simple rule relates the generalized cross section σ to the irradiance I_s at the break and an effective pulse length T_p which is 700 fs in this case, according to $\sigma I_s^3 T_p = 1$. When $I_s = 100$ TW/cm^2, this estimates $\sigma = 2 \times 10^{-48}$ cm^{6}W^{-2}. One must take I_s to be 20 TW/cm^2 to bring σ into the range of perturbation-theory calculations.

If one tries to match the experiment to the perturbative and Floquet predictions by assuming that a single parameter was measured incorrectly, that parameter must be the waist radius of the laser beam. The other parameters would have to be adjusted far beyond the estimated uncertainties. For example, the pulse duration must be longer by a factor of 3, or the hydrogen density lower by a factor of 25, to match the perturbative calculations. However, both the predicted electron counts and the calculated irradiances of the experimental points depend on the waist radius. The measurements can be brought into agreement with the Coulomb-Keldysh calculations by taking the waist radius of the laser beam to be 30% larger (45 μm rather than 35 μm). This change is within the estimated uncertainties. Achieving the same agreement would require increasing the pulse length or joulemeter calibration

by 40%, or decreasing the gas density or detection efficiency by a factor of 2.8. Much larger changes would be required to match the other models, such as $W_0=75$ μm to reach the perturbative and Floquet models, or $W_0=20$ μm for the Reiss and Keldysh models.

In conclusion, the perturbative and Floquet calculations predict larger electron counts than were measured. The Coulomb-corrected Keldysh model is in better agreement. The widely used Reiss and Keldysh methods underestimate the rates by a large factor. These should not be used to estimate rates of plasma heating by multiphoton ionization.

We acknowledge the help of Dr. D. Casperson in the design of the electron TOF spectrometer and the help of M. Maestas, K. Stetler, and S. Harper in the laboratory. This work was performed under the auspices of the U.S. Department of Energy under Contract No. W-7405-ENG-36.

[1] L. V. Keldysh, Zh. Eksp. Teor. Fiz. **47**, 1945 (1964) [Sov. Phys. JETP **20**, 1307 (1965)].
[2] E. Karule, *Atomic Processes* (Latvian Acad. Sci., Riga, 1975), p. 5 (in Russian).
[3] S. V. Khristenko and S. I. Vetchinkin, Opt. Specktrosk. **40**, 417 (1976) [Opt. Spectrosc. **40**, 239 (1976)].
[4] G. Laplanche, A. Durrieu, Y. Flank, M. Jaouen, and A. Rachman, J. Phys. B **9**, 1263 (1976).
[5] A. Maquet, Phys. Rev. A **15**, 1088 (1977).
[6] H. R. Reiss, Phys. Rev. A **22**, 1786 (1980).
[7] S.-I. Chu and J. Cooper, Phys. Rev. A **32**, 2769 (1985); S.-I. Chu (private communication).
[8] H. R. Reiss, J. Opt. Soc. Am. B **4**, 726 (1987).
[9] B. Gao and A. F. Starace, Phys. Rev. Lett. **61**, 404 (1988).
[10] B. Gao and A. F. Starace, Phys. Rev. A **39**, 4550 (1989).
[11] K. J. Lagattuta, Phys. Rev. A **41**, 5110 (1990).
[12] M. S. Pindzola, Bull. Am. Phys. Soc. **35(5)**, 1151 (1990); M. S. Pindzola and Martin Dörr, Phys. Rev. A **43**, 439 (1991).
[13] P. B. Corkum, N. H. Burnett, and F. Brunel, Phys. Rev. Lett. **62**, 1259 (1989).
[14] M. LuVan, G. Mainfray, C. Manus, and I. Tugov, Phys. Rev. A **7**, 91 (1973).
[15] D. E. Kelleher, M. Ligare, and L. Brewer, Phys. Rev. A **31**, 2747 (1985).
[16] H. G. Muller, H. B. van Linden van den Heuvell, and M. J. van der Wiel, Phys. Rev. A **34**, 236 (1986).
[17] D. Feldmann, B. Wolff, M. Wemhoener, and K. H. Welge, Z. Phys. D **6**, 293 (1987); B. Wolff, H. Rottke, D. Feldmann, and K. H. Welge, *ibid.* **10**, 35 (1988); H. Rottke, B. Wolff, M. Brickwedde, D. Feldmann, and K. H. Welge, Phys. Rev. Lett. **64**, 404 (1990).
[18] J. Slevin and W. Stirling, Rev. Sci. Instrum. **52**, 1780 (1981).
[19] P. Kruit and F. H. Read, J. Phys. E **16**, 313 (1983).
[20] J. P. Roberts, A. J. Taylor, P. H. Y. Lee, and R. B. Gibson, Opt. Lett. **13**, 734 (1988).
[21] L. Marshall, Laser Focus **7** (4), 26 (1971).
[22] M. R. Cervenan and N. R. Isenor, Opt. Commun. **13**, 175 (1975).